Journal of Magnetics 1 (1), 31-36 (1996)

Enhanced Exchange Coupling of $Nd_2Fe_{14}B/Fe_3B$ Magnet Via Magnetic Field Treatment

Choong Jin Yang and Eon Byung Park

Electromagnetic Materials Lab., Research Institute of Industrial Science & Technology (RIST), P. O. Box 135, 790-330 Pohang, Korea

(Received 13 May 1996)

An externally applied magnetic field during heat treating the $Nd_2Fe_{14}B/Fe_3B$ based spring magnet was found to enhance the exchange coupling between the hard and soft magnetic grains. More than 30 % increase in M_r/M_s values for melt-spun $Nd_4Fe_{73.5}Co_3(Hf_{1-x}Ga_x)B_{18.5}$ (x = 0, 0.5, 1) alloys was resulted from a uniform distribution of Fe_3B, α-Fe and $Nd_2Fe_{14}B$ phases, and also from a reduced grain size of those phases by 20 %. The externally applied magnetic field induced a uniform distribution of fine grains. A study of Mössbauer effect also report that the enhancement of total magnetization of nanocomposite $Nd_2Fe_{14}B/Fe_3B$ alloys is attributed to an increased formation of Fe_3B after magnetic annealing.

1. Introduction

Nanocomposite spring magnets provide an alternate way to produce a high remanence magnetic materials which can be made into resin bonded magnets. Additional merit is in the cost reduction due to the less use of rare earth element. Basically the nanocomposite magnets have been studied on the compostion of $Nd_2Fe_{14}B/Fe_3B$ [1, 2] and $Nd_2Fe_{14}B/\alpha$-Fe [3, 4]. Although those magnetic materials showed M_r/M_s values (≤ 0.8) higher than the Stoner-Wohlfarth limitation ($M_r/M_s = 0.5$), the obtainable coercivity is still very low ranging over 2~4 kOe [5, 6].

According to the nanocomposite model proposed by Kneller & Hawig [7], the exchange coupling takes place when the critical particle size of both the soft (b_{cm}) and hard (b_{ck}) magnetic phases satisfies the relationship $b_{cm} = \pi (A_k/2K_k)^{1/2} = b_{ck}$ where A_k is anisotropic energy and K_k is anisotropic constant. The computed size resulted in 10 nm for $Nd_2Fe_{14}B/\alpha$-Fe magnets. Realistically, however, the order of formation of $Nd_2Fe_{14}B$, Fe_3B and α-Fe is different, and the growth rate during phase separation is not the same. Despite the realisitc fact, the previously reported studies were focussed on an interest in grain size reduction via a rapid soidification technique which has not guaranteed the effective exchange coupling yet. Recently, Fukunaga et al [8, 9]. reported results of computer simulation that there is an optimum grain size exhibiting a maximized energy product being dependent upon the volume fraction of soft (or hard) phase. The coupling force influences not only on the remanence magnetization but sometimes causes a decrease in coercivity below a certain grain size. In his computer simulation, however, the so called exchange energy parameter ($= SJ_e/6KV$) was used on the assumption that the grains are with identical shape therefore disregarding the magnetostatic energy. S and V are the surface area and volume of $Nd_2Fe_{14}B$ grains, respectively, and J_e is the exchange coupling constant.

The present study reports an additional result of Mössbauer effect on the nanocomposite magnets which showed an significantly enhanced remanence ratios induced by a uniform distribution of fine grains caused by the external magetic field [10].

2. Experimental

Ingots of $Nd_4Fe_{73.5}Co_3(Hf_{1-x}Ga_x)B_{18.5}$ (x = 0, 0.5, 1) composition were prepared by plasma arc-melting the costituent elements in an argon atmosphere. 50~60 g pieces of ingot were melt-spun from a quartz tube, and spun onto a rotating wheel at a speed of 40 m/sec. The amorphous ribbons obtained were 20~30 μm thick and 10~15mm wide. These samples were annealed by furnace annealing as well as magnetic field annealing at 650~710 ℃ for 5 minutes. The applied field was fixed at 5 kOe along the direction of ribbon's long axis. X-ray diffraction of Cu Kα radiation was used to identify the phases present, and microstructure and composition were checked by a transmission electron microscope. The hysteresis loops were measured in a vibrating sample magnetometer with a maximum field of 19 kOe along the long axis using appropriate demagnetization factors. Morphology of fracture surface image analysing were carried out using an image scanner attached in a scanning electron microscope. Additional thermomagnetic behaviors were examined using a thermogravimetric analyzer to identify the magnetic transformation of amorphous ribbons. Room temperature

Mössbauer spectroscopy was carried out without applying a magnetic field using ^{57}Co (Rh) source for the ribbon samples to monitor the volume fraction of each phase formed during annealing.

3. Results and Discussion

A. The Typical Magnetic Properties After Furnace Annealing

When the spring magnets consisted of Fe_3B and /or α-Fe with the hard phase $Nd_2Fe_{14}B$ are not heat treated properly, they always show hysteresis curves having a constriction at H = 0 as shown in Fig. 1. All the compositions used in this study

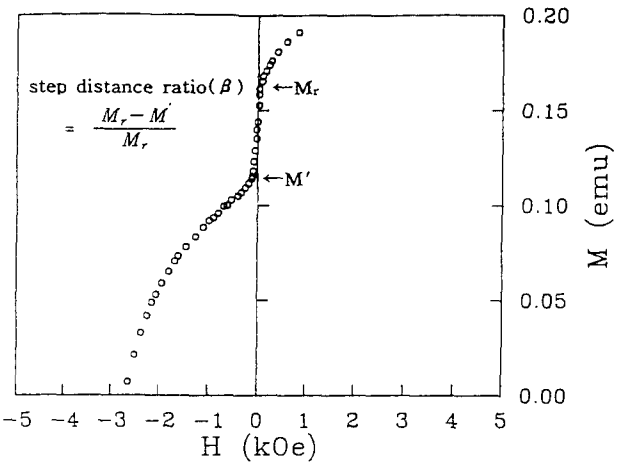

Fig. 1 The typical hysteresis loop of melt-spun $Nd_4Fe_{73.5}Co_3Hf_{0.5}Ga_{0.5}B_{18.5}$ ribbons after annealing at 680 ℃ for 5 minutes without a magetic field.

showed the same behaviors. This is due to the lack of full exchange coupling between the soft and hard phases leading to a low remanence magnetization. We have defined a "step distance ratio (STR)" as $(M_r\text{-}M')/M_r$ in this study for every samples, and plotted the STR and M_r/M_s as a function of annealing temperature as shown in Fig. 2. The STR increases with increasing annealing temperature for all the compositions, accordingly M_r/M_s shows decreases. $Nd_4Fe_{73.5}Co_3Hf_{0.5}Ga_{0.5}B_{18.5}$ alloy shows the superior properties to those of others. Accordingly the effect of the addition of Hf and Ga was examined as plotted in Fig. 3. M_r/M_s ratio evidently increases with the additon of Ga and Hf at the same time exhibiting peak vaslues for all the annealing temepratures at x (Ga) = 0.5, and decreases thereafter. At low annealing temperature except 705 ℃, however, the STR shows relatively consistant values. The addition of Ga is believed to enhance M_r/M_s values caused by the grain refinment. But the grain refinement by Ga may be superimopsed on the effect of temperature at a low annealing range. This is why the STR values at lower temperature are relatively consistant, and high M_r/M_s ratios are obtained by annealing at 628 ℃ for 5 minutes.

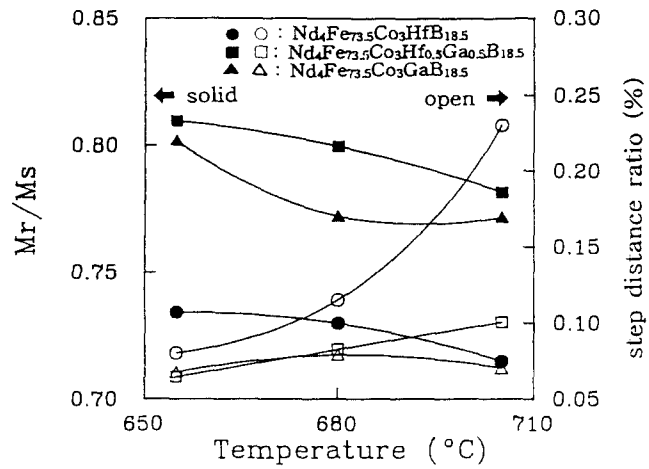

Fig. 2 Variation of reduced remanence (M_r/M_s) and step distance ratio ($(M_r/M')/M_r$) of the melt-spun $Nd_4Fe_{73.5}Co_3Hf_{1-x}Ga_xB_{18.5}$ (x = 0, 0.5, 1) ribbons as a function of annealing temperature.

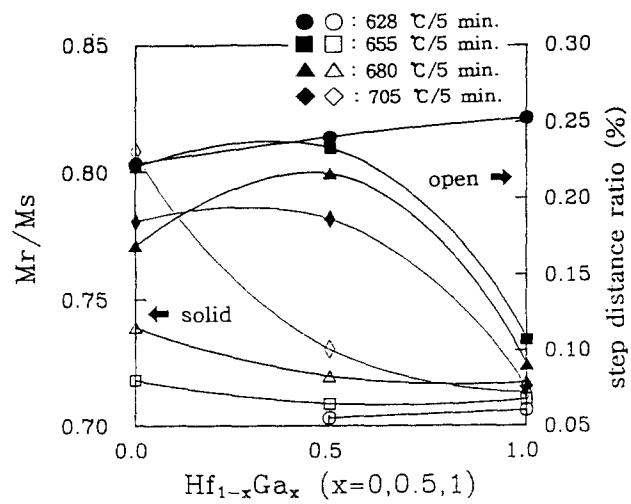

Fig. 3. Variation of reduced remanence (M_r/M_s) and step distance ratio ($(M_r/M')/M_r$) of the melt-spun $Nd_4Fe_{73.5}Co_3Hf_{1-x}Ga_xB_{18.5}$ (x = 0, 0.5,1) ribbons as a function of Hf content (x) after annealing.

B. Enhanced Magnetic Properties After Annealing In a Magnetic Field

Fig. 4 demonstartes the effect of external magetic field on the enhanced remanence magnetization and energy product as well. Both the remanence magnetization and energy product values were obtained to be enhanced by 20~30% for all the compositions, though $Nd_4Fe_{73.5}Co_3GaB_{18.5}$ alloys show the least effects, examined by applying an external field of 5 kOe during annealing the melt-spun alloys. Particularly the $Nd_4Fe_{73.5}Co_3Hf_{0.5}Ga_{0.5}B_{18.5}$ alloy exhibits the energy product of 15.8 MGOe resulted from the high remanence (12.6 kG) and coercivity (2.8 kOe) as well at the annealing temperature of 680 ℃. It is of interest to note that the coercivity values of $Nd_4Fe_{73.5}Co_3Hf_{0.5}Ga_{0.5}B_{18.5}$ and $Nd_4Fe_{73.5}Co_3HfB_{18.5}$ alloys show

the maximum values at 680 ℃, and then tend to drop above that temperature.

Fukunaka et al. [8, 9] claimed that the magnetostatic energy does not play any influence on exchange coupling between two phases, and the coupling force increases with decreasing the grain size. However, they showed the behavior of coercivity as a function of grain size that the coercivity reach a maximum value when the exchange coupling parameter [9], J_cS/K_uV, drops just below 1. The parameter 1 corresponds to $(S/V)^{-1}=20$ nm in his report for $Nd_2Fe_{14}B$ based composite. When $J_cS/K_uV>1$, the coercivity was almost zero. He explained the behavior in terms of isotropic properties where the degree of isotropy increases with decreasing the grain size. Fig. 4 shows the identical trend with his simulation such that the magnetic annealing at 680 ℃ exhibited a peak coercivity of 2.83 kOe with the grain size of 22 nm. The coercivity drops above 705 ℃ seems to be caused by grain coarsening, while the low values in coercivity at 655 ℃ is due to too fine grain size.

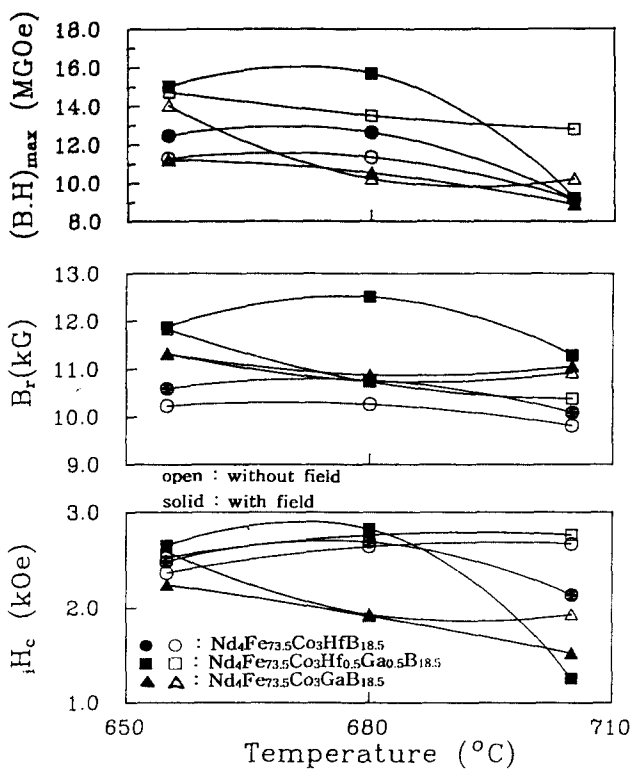

Fig. 4 Variation of magnetic properties of the melt-spun $Nd_4Fe_{73.5}Co_3Hf_{1-x}Ga_xB_{18.5}$ (x=0, 0.5, 1) ribbons as a function of annealing temperature with and without a magnetic field.

Fig. 5 shows the typical hysteresis curves before and after the magnetic annealing where the enhancement in M_r/M_s is prominent. The enhanced properties are plotted in Fig. 6 where all the three composition demnonstrates a 20~30% increase in M_r/M_s values. The $Nd_4Fe_{73.5}Co_3Hf_{0.5}Ga_{0.5}B_{18.5}$ alloys always exhibited M_r/M_s values more than 0.82 which is considerably hard to obtain by convential ways. Besides the M_r/M_s of that alloy was

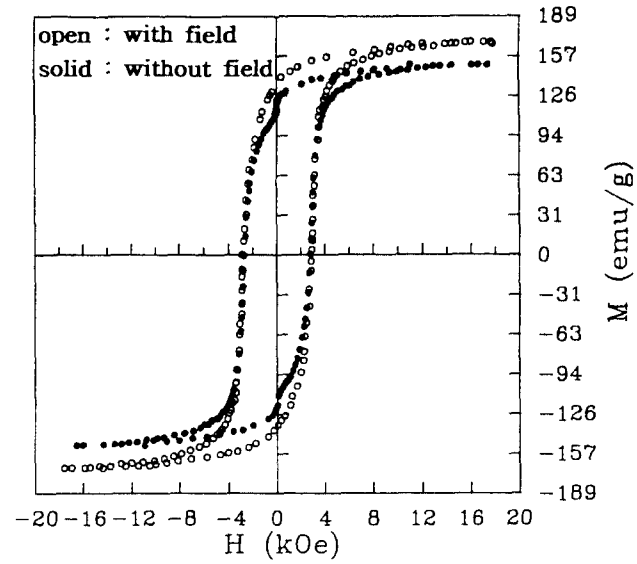

Fig. 5 The typcal hysteresis loops of melt-spun $Nd_4Fe_{73.5}Co_3Hf_{0.5}Ga_{0.5}B_{18.5}$ ribbons after annealing with and without a magnetic field.

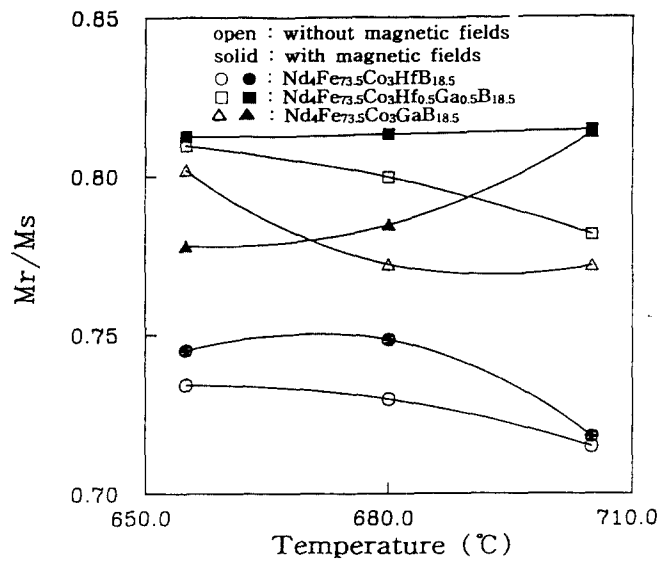

Fig. 6 Variation of reduced remanence (M_r/M_s) of the melt-spun $Nd_4Fe_{73.5}Co_3Hf_{1-x}Ga_xB_{18.5}$ (x=0, 0.5, 1) ribbons as a function of annealing with and without a magnetic field.

found not to be influenced by a high annealing temperature.

Taking into account the X-ray diffraction pattrens of $Nd_4Fe_{73.5}Co_3Hf_{0.5}$-$Ga_{0.5}B_{18.5}$ in Fig. 7, one will realize that considerable changes took place for α-Fe and Fe_3B phases after the annealing without and with a magnetic field. (110) and (200) peaks of α-Fe can be seen to be diffused with a shortened height after the annealing with a magnetic field. This is the same for (301), (311), (321), (302) and (411) of Fe_3B. On the other hand no change is observed for $Nd_2Fe_{14}B$ peaks. The observed lattice parameters of each phase are a=2.8779 for α-Fe, a=8.

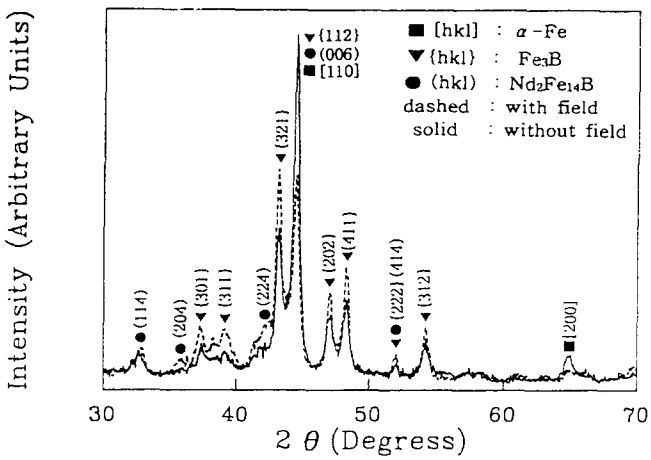

Fig. 7 X-ray diffraction patterns of melt-spun $Nd_4Fe_{73.5}Co_3Hf_{0.5}Ga_{0.5}B_{18.5}$ ribbons after annealing with and without a magnetic field.

6832 and c=4.2835 for Fe_3B and a=8.7875 and c=12.21 Å for $Nd_2Fe_{14}B$, respectively. The $Nd_4Fe_{73.5}Co_3GaB_{18.5}$ and $Nd_4Fe_{73.5}Co_3HfB_{18.5}$ alloys also showed the identical patterns indicating that grains become finer by applying the external field. In order to relate this change in patterns with microstructures, we confirmed the grain refinment by scanning 1000 grains using the transmission electron microscopy and an image analyzer attached in a scanning electron microsope as shown in Fig. 8 and Fig. 9, respectively. Magnetic annealing without a field as shown in Fig. 8 (a) and (b) introduced abnormally coarse α-Fe (particles appearing black) and Fe_3B grains with an average grain size of 30 nm. After the magnetic annealing, however,

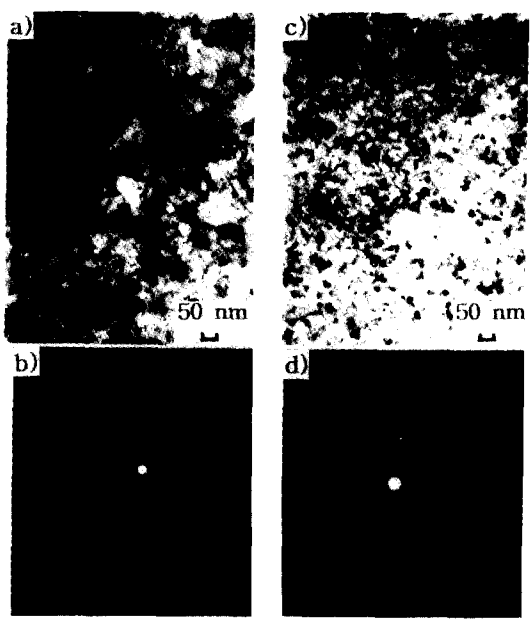

Fig. 8 TEM micrographs showing the grain aspect of the annealed $Nd_4Fe_{73.5}Co_3Ga_{0.5}Hf_{0.5}B_{18.5}$ ribbons (a) without a magnetic field and its (b) selected area diffraction pattern, (c) with a magnetic field and its (d) selected area diffraction pattern.

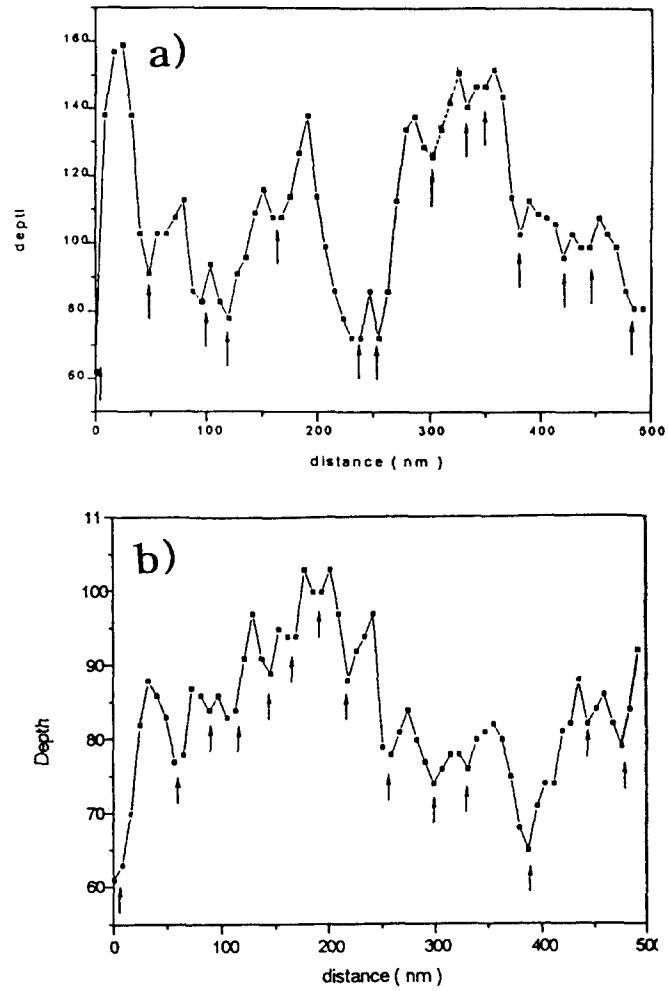

Fig. 9 Grain size distribution for the annealed ribbons (a) without a magnetic field, and (b) with a magnetic field corresponding to Fig. 8.

very uniform distribution of fine grains were obtained being evident in Fig. 8 (c) and (d). The uniformity of grains for each case is idnetified by scanning 1000 grains and shown in Fig. 9 (a) and (b). The grain irregularity (size scattering) of 70~160% was measured before the magnetic annealing, while the irregularity of 60~100% was obtained after the annealing. Considering the enhancement in M_r/M_s values, X-ray patterns and the results of grain aspect, applying an external field during annealing induces not only the grain refinment but causes a uniform distribution of the grains at the same time. Presently the exact mechanism of grain refinment is not known yet.

Fig. 10 (a) and (b) show the Mössbauer spectra at room temperature for the $Nd_4Fe_{73.5}Co_3Hf_{0.5}Ga_{0.5}B_{18.5}$ samples annealed without and with a magnetic field. The curves of solid circles are as measured, and the curves of different colors correspond to resolved fits of each aomic site of existing phases. One can find that both the spectra of annealed sample without and with a magnetic field are fitted well with subspectra for each α-Fe, Fe_3B, and $Nd_2Fe_{14}B$. The amorphous samples annealed without or with a field at 680 ℃ for 5 minutes, which is the optimal

condition to obtain the best hard magnetic properties, consist of mainly bct-Fe_3B (67~82 vol. %), and then α-Fe (6~19 vol. %), and small amount of $Nd_2Fe_{14}B$ (12~14 vol. %). These volume contents of soft and hard magnetic phases in the $Nd_4Fe_{73.5}Co_3Hf_{0.5}Ga_{0.5}B_{18.5}$ alloy are very close to those of simulated model proposed by Kneller and Hawig [7] who proposed 10 vol. % of hard magnetic phase when the critical grain size for each soft and hard magnetic phase is identical to obtain the appropriate exchange coupling.

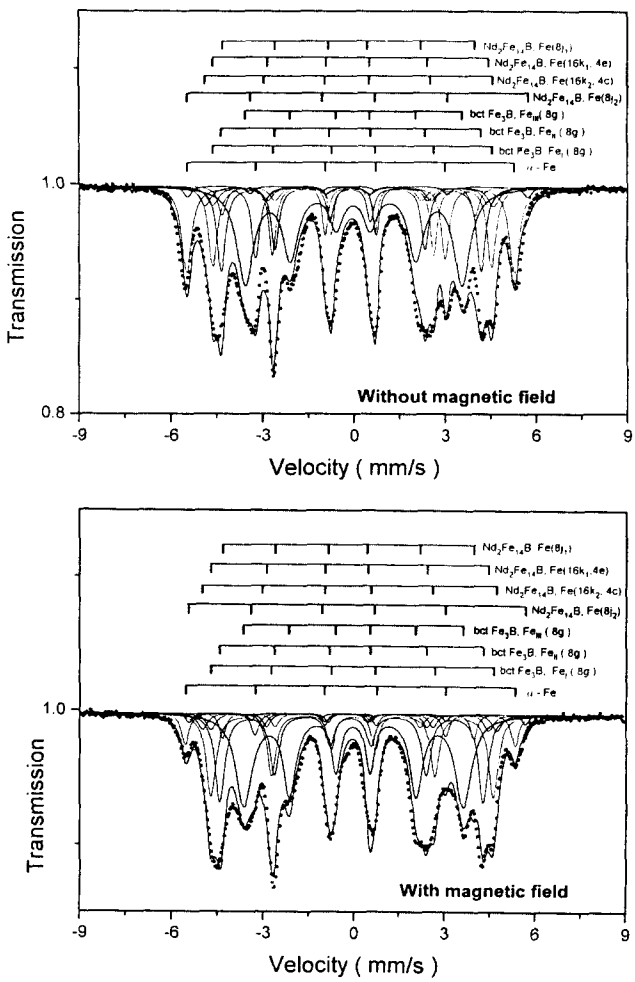

Fig. 10 The resolved curve fits of α-Fe, Fe_3B and $Nd_2Fe_{14}B$ phases of Mössbauer spectroscopy for (a) the alloys annealed without a magnetic field, and (b) with a field.

The result of Mössbauer spectroscopy is summarized in Table I. Basically the changes in hyperfine field (HF), isomer shift (IS), and quadrupole splitting (QD) for each phase in the sample annealed without and with a magnetic field are not prominent. In general, however, a reduced IS and QD, and an increased HF are obtained by annealing the samples at a magnetic field. This result implies that magnetically treated nanocomposite alloys induced a well developed long range ordering in Fe_3B and $Nd_2Fe_{14}B$ structures taking into account the increased HF and reduced IS/QD for Fe_3B particularly. Most of all, it is worthy to note that the volume fraction of Fe_3B increases from 67.21 % to 82.08 % while that of α-Fe decreases from 18.94 % to 6.22 %. The formation of $Nd_2Fe_{14}B$ phase slightly decrease from 13.85 to 11.72 vol. %. Therefore it is proposed that the enhancement in reduced remanence ($M_r/M_s = 0.82$) in this alloy was induced also by the increased formation of Fe_3B phase in addition to the effect of grain refinment during the magnetic annealing. The tetragonal Fe_3B consisting of 8 formula units of trigonal prism has three inequivalent Fe sites Fe_I (8 g), Fe_{II} (8 g) and Fe_{III} (8 g) at the vertices of trigonal prism [11]. The Fe_I (8 g) was reported to have an atomic moment of 2.03 μ_B, and also has 10 nearest neighbors. Accordingly one can claim that the increased formation of Fe_3B contribute to the enhancement of total magnetization of the nanocomposite magnets. From the present Mössbauer spectroscopy average HF of the Fe_I (8 g) atoms was measured to be 28.99 Tesla which is quite similar to that of Mao's report [12], but smaller than that of single phase Fe_3B [13].

In conclusion, an external magnetic field during annealing the melt-spun $Nd_4Fe_{73.5}Co_3(Hf_{1-x}Ga_x)B_{18.5}$ ($x = 0$, 0.5, 1) alloys was found to induce a grain refinment about 20 % and enhances

Table I. The result of Mössbauer spectroscopy

phase/site		HF (T)	I. S (mm/sec)	Q. D (mm/sec)	Vol. fraction(%)
α-Fe	without field	33.43	−0.114	0.010	18.94
	with field	33.85	−0.116	0.009	6.22
bct Fe_3B $Fe_{(I)}$ (8 g)	without field	28.43	−0.046	−0.012	
	with field	28.99	−0.037	−0.015	67.21
bct Fe_3B $Fe_{(II)}$ (8 g)	without field	26.45	−0.122	0.042	
	with field	26.98	−0.103	0.046	
bct Fe_3B $Fe_{(III)}$ (8 g)	without field	22.12	−0.0301	0.021	82.08
	with field	22.52	−0.027	0.023	
$Nd_2Fe_{14}B$ $Fe(8j_2)$	without field	34.73	−0.033	0.310	
	with field	34.51	−0.032	0.303	13.854
$Nd_2Fe_{14}B$ $Fe(16k_1, 4e)$	without field	28.21	−0.165	0.121	
	with field	28.51	−0.182	0.120	
$Nd_2Fe_{14}B$ $Fe(16k_2, 4c)$	without field	29.41	−0.192	0.071	
	with field	30.21	−0.161	0.082	
$Nd_2Fe_{14}B$ $Fe(8j_1)$	without field	25.82	−0.192	0.033	11.72
	with field	25.80	−0.194	0.03	

remanence/energy product values by 30%. The magetic field also causes a uniform distribution of α-Fe and Fe_3B grains, and an increased formation of Fe_3B phase during annealing. The alloys at $x = 0.5$ exhibited the remanence magnetization of 12.5 kG and $(B.H)_{max}$ of 15.8 MGOe with a coercivity of 2.83 kOe. At this composition the grain size was observed to be 22 nm.

References

[1] R. Coehoorn, D. B. De Mooij and C. De Waard, J. Magn. Mag. Mater. **80** (1989) 101.
[2] J. Ding, P. G. McCormick and R. Street, J. Magn. Mag. Mater. **124** (1993) 1.
[3] A. Manaf, R. A. Buckely and H. A. Davies, J. Magn. Mag. Mater. **128** (1993) 302.
[4] J. Wecker, K. Schnitzke and H. Cerva, Appl. Phys. Lett. **67** (4) (1995) 563.
[5] L. Withanawasam and G. C. Hadjipanayis, J. Appl. Phys. **76** (10) (1994) 7065.
[6] J. M. Yao, T. S. Chin and S. K. Chen, J. Appl. Phys. **76** (10) (1994) 7071.
[7] E. F. Kneller and R. Hawig, IEEE Trans. on Mag. **27** (4) (1991) 3588.
[8] H. Fukunaga and H. Inoue, Jap. J. Appl. Phys. **31** (1992) 1347.
[9] N. Kitajima and H. Fukunaga, Proc. 3rd Inter. Symposium on Phys. of Mag. Mater., ed. by C. S. Kim and T. D. Lee, (The Korean Magnetic Society, Seoul, Korea, Aug. 21-25, 1995), p. 652-655.
[10] C. J. Yang and Y. B. Park, ***ibid***, p. 675-678.
[11] Y. D. Zhang J. I. Budnick, J. C. Ford and W. A. Hines, J. Magn. Mag. Mater. **100** (1991) 13.
[12] M. Mao, C. Yang and F. Li, J. Phys.: Condens. Matter. **4** (1992) 9147.
[13] C. L. Chien, D. Musser, F. E. Luborsky and J. L. Water, Phys. Rev. B **20** (1979) 283.